

# OFF-SHORE WIND FIELDS OBTAINED FROM MESOSCALE MODELING AND SATELLITE SAR IMAGES

B. H. Jørgensen<sup>†</sup>, B. Furevik<sup>\*</sup>, C. B. Hasager<sup>†</sup>, P. Astrup<sup>†</sup>, O. Rathmann<sup>†</sup>, R. Barthelme<sup>†</sup>, S. Pryor<sup>†</sup>

<sup>†</sup>Risø National Laboratory, Wind Energy Department,  
DK-4000 Roskilde, Denmark, Phone +45 4677 5471 / Fax +45 4677 5970; bo.hoffmann@risoe.dk

<sup>\*</sup>Nansen Environmental and Remote Sensing Center  
Edvard Griegsvei 3A, N-5059 Bergen, Norway. Phone +47 55297288, Fax +47 5520 0050

**ABSTRACT:** The wind field in coastal regions is simulated with the Karlsruhe Atmospheric Mesoscale Model 2 (KAMM2). Data (4 times daily) from the global reanalysis of NCEP/NCAR is used to obtain the geostrophic wind and other large scale forcings which are suitable as input to the mesoscale model. The results of the simulations are compared with wind fields derived from satellite Synthetic Aperture Radar (SAR) images and results from the Linearized Computational Model (LINCOS) of Risø National Laboratory. SAR images provide ocean wind speed maps with a 400 m spatial resolution covering areas of 100 km \* 100 km as snap-shots 3 times a month, thus offering a unique possibility of evaluating the performance of the mesoscale model at a relatively low cost. The SAR-derived wind speed is obtained from radar backscatter due to the water roughness generated by the interaction between the wind and capillary and short gravity waves. In fetch-limited seas additional parameters may influence the roughness of the sea as compared to that of the open sea. However, the current empirical algorithms used for obtaining the wind speed from the backscatter are calibrated for the open sea. Therefore, the mesoscale model and data from LINCOS are useful for comparison with the SAR-derived wind speeds close to the shore.

**Keywords:** Off-shore, wind, boundary layer, mesoscale model

## 1 INTRODUCTION

### 1.1 Background

Offshore wind resources are today predicted from at least one year of wind observations at meteorological masts positioned in the sea or at the coastline. Alternatively, mesoscale modeling using large scale forcing derived from reanalysis data can be used to calculate the wind field. However, most of the experience with mesoscale modeling of wind resources is based on calculations for land regions rather than at sea. Satellite wind speed maps may provide new information relevant for offshore wind parks at a relatively low cost.

We have performed calculations with the non-hydrostatic Karlsruhe Atmospheric Mesoscale Model 2 (KAMM2) in order to validate the SAR derived wind speed maps near coast line. In addition, we are using the SAR image to evaluate the performance of the mesoscale model far from the coast line.

Satellite images from Synthetic Aperture Radar (SAR) can be processed to provide maps of ocean wind speed. The data are of a high spatial resolution sampled three times a month. Radar looks through clouds and rain, so it works in all weather conditions.

Data used in the current work consists of 16 cases containing a total of 20 scenes originating from the ERS SAR system providing images of backscatter coefficients that are used to calculate wind speed and direction in a 100 km \* 100 km area. The location under study is the Horns Rev offshore site in Denmark where ELSAM/ELTRA is planning a large wind farm [1].

### 1.2 SAR based wind climate estimation

It is expected that large ensembles of SAR images can be used to estimate off-shore wind climates. The main disadvantage is the low temporal coverage, however,

comparison with measurement data indicate that relatively few scenes (50-100) selected randomly from once per day satellite images should give the mean wind speed with a mean absolute error of less than 10% (disregarding algorithm error and provided that the diurnal cycle of wind speeds is small or well-represented by the sampling).

## 2 THE MODELS

### 2.1 The mesoscale model KAMM2

The Karlsruhe Atmospheric Mesoscale Model 2 (KAMM2) is a three-dimensional, non-hydrostatic, and compressible meso-scale model [2] related to KAMM [3,4]. Spatial derivatives are calculated in the model by central differences on a terrain following grid. The turbulent fluxes are parameterized using a mixing-length model with stability dependent turbulent diffusion coefficients in stably stratified flow, and a non-local closure for the convective mixed layer. Advection is calculated using a flux corrected transport algorithm. Lateral boundary conditions assume zero gradients normal to the inflow sides. On outflow boundaries, the horizontal equations of motion are replaced by a simple wave equation allowing signals to pass out of the domain without reflection. Gravity waves are absorbed in the upper part of the computational domain which acts as a damping layer. The model has been extended with a fetch-dependent sea roughness [5]. At initialization, the orography (see Figure 1), roughness, and large scale forcing (see 2.2) is loaded into the model.

The present calculations for Horns Rev have mainly been performed with a grid containing 121\*121\*51 cells for an area which is 120 km\*120 km, i.e. 1 km horizontal resolution. A few runs with 500 m and 2 km resolution have been performed to ensure grid independence.

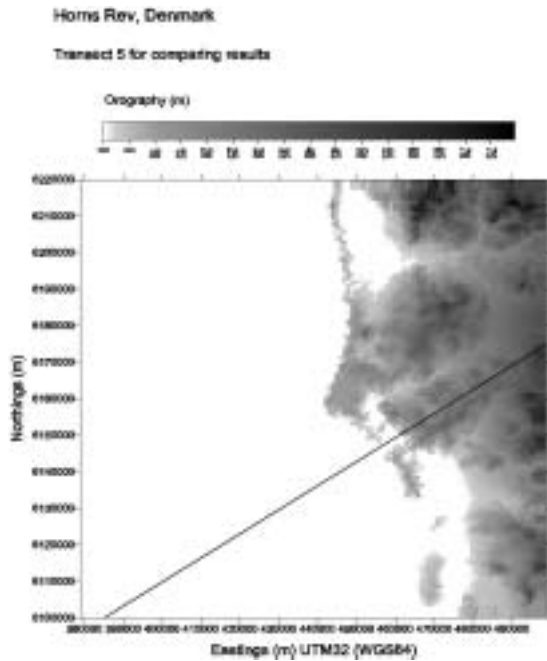


**Figure 1.** Orography near Horns Rev, Denmark used in the mesoscale model and LINCOM. A transect proceeding from the sea towards land is depicted.

## 2.2 Large-scale forcing

Data (4 times daily) from the global reanalysis of NCEP/NCAR [6] is used to obtain the geostrophic wind and other large scale forcing (vertical air temperature gradient, air temperature at 2 m height, and temperature at land and sea) which is suitable as input to the meso-scale model. KAMM2 is able to run as a “stand-alone” model, i.e. the model can be run by using only the large scale forcing from the reanalysis (see sketch in Figure 2). Hence, it is not necessary to nest the meso-scale model within a larger model supplying the boundary conditions. For each case, the time of the reanalysis data is chosen as close as possible to the time of the satellite overpassing.

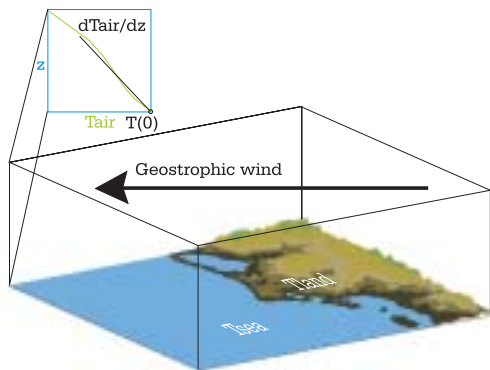


**Figure 2.** Sketch of the large scale forcing used for KAMM2 calculations.

## 2.3 The local scale LINCOM model

LINCOM [7,8] is a linear spectral wind flow model for slightly complex terrain. Based on the orography and roughness, it calculates the perturbations induced in a known background flow that is otherwise in equilibrium with a flat area with uniform roughness. The sum of the

perturbations and background flow gives the final flow field.

While the orography and the roughness over land are fixed, sea roughness is a function of the wind, and therefore of the output. In order to obtain a more realistic response for the wind over sea, LINCOM includes a model for the sea roughness [8]. An iterative procedure leads to a wind field and a sea roughness field in balance with each other.

The background flow in the current work is obtained from wind speed measurements at 62 m height of the Horns Rev meteorological mast. The LINCOM results at 10m height is used for indicating the local levels of the wind speed in comparison with the other data sets.

## 3 THE SATELLITE AND MAST DATA

### 3.1 Satellite SAR images

Satellite SAR data are available from the European ERS-2 and the Canadian RADARSAT-1. These SAR sensors are C-band (wavelength around 5 cm).

ERS SAR data have a repeat track of about 10 days and a 100 km swath. Hence, the area of each scene is viewed approximately three times per month (at mid-latitudes). Each scene is 100 km \* 100 km and the raw resolution of the cells is 30 m \* 30 m.

The measured quantity in each resolution cell is the backscatter coefficient (the normalised radar cross section), which is dependent upon the relative wind direction (zero for a wind blowing against the radar), the local radar beam incidence angle of the target area and the wind speed. This is described in Hasager *et al.* [9].

The SAR wind speed retrieval method originates from C-band scatterometer model CMOD-IFR2 [10], which is based on correlation analysis between global ocean buoy data and C-band scatterometer data. The ERS SAR wind maps are produced under the assumption that the wind directions are known from observations at the mast at Horns Rev.

The model coefficients depend on the incidence angle and wind speed given by look-up tables [10]. The typical resulting accuracy, solving for wind direction, is  $\pm 20^\circ$  and, solving for wind speed,  $2 \text{ m s}^{-1}$  or 10% (RMS) for wind speeds between  $2\text{-}24 \text{ m s}^{-1}$  [11]. The wind speed is derived for a nominal height of 10 m above sea level.

The physical principle of C-band SAR backscatter coefficients and wind speed is given through the aerodynamic roughness (surface stress). The SAR-derived wind speed is obtained from radar backscatter due to the water roughness generated by the interaction between the wind and capillary and short gravity waves. In fetch-limited seas additional parameters may influence the roughness of the sea as compared to that of the open sea, in particular due to wave age, water depth, tidal currents, and atmospheric stability. However, the current CMOD algorithms used for obtaining the wind speed from the backscatter are calibrated for open sea conditions.

### 3.2 Selection of SAR images to describe climatology

Satellite SAR data was selected to represent the relevant wind climatology for the Horns Rev site. Out of a total of 32 SAR scenes recorded from the site within one year covering May 1999 to May 2000, a series of 20 scenes covering 16 dates were obtained from the European Space Agency.

The data set contains wind speed data in three regimes: low ( $3 - 9 \text{ m s}^{-1}$ ) 7 cases, medium ( $9 - 13 \text{ m s}^{-1}$ ) 5 cases and high ( $13 - 18 \text{ m s}^{-1}$ ) 4 cases. The cases cover 4 offshore, 4 along-shore and 8 onshore situations. The data set is listed in Table I.

### 3.3 Offshore mast observations at Horns Rev

At Horns Rev, Denmark, a 62 m tall meteorological tower positioned 14 km offshore west of the coast of Jutland has been equipped with wind speed, wind direction and temperature sensors since May 1999 [1] by ELSAM/ELTRA. These data have been analysed to yield the hourly mean wind speed at 10 m (assuming a logarithmic wind profile) and wind direction in listed in Table I. Also listed in the table are wind speeds extracted from the SAR scenes near the location of the mast. With the exception of one obvious error and two other cases the SAR derived wind speeds are within the prescribed error limits of  $\pm 2 \text{ m/s}$  for wind speeds above  $5 \text{ m/s}$ . For wind speeds below  $5 \text{ m/s}$  the present SAR data do not appear to reproduce the insitu measurements.

**Table I:** Dates of ERS SAR scenes from Horns Rev, wind speed at 10 m and wind direction at 60 m as hourly mean values from the mast, and corresponding wind speed at 10 m from SAR scenes.

Case	Date	Time (UTC)	Dir (deg) Mast	U (m/s) Mast	U (m/s) SAR
1	19990520	21:30	122.3	7.8	1.69
2	19990621	21:24	313.9	10.1	8.98
3	19990710	20:57	71.8	4.2	1.80
4	19990729	21:30	34.9	5.6	5.49
5	19990810	10:30	328.8	11.2	8.77
6	19990830	21:24	291.8	7.0	6.19
7	19991003	10:30	240.8	11.9	8.60
8	19991007	21:30	274.4	10.4	9.37
9	19991019	10:30	88.8	8.9	8.39
10	19991123	10:30	233.3	1.6	0.47
11	19991216	21:30	244.3	9.9	9.48
12	20000116	10:30	305.6	7.7	6.80
13	20000201	10:30	235.1	10.5	9.69
14	20000307	10:28	256.3	12.2	11.40
15	20000326	10:31	125.6	4.3	1.46
16	20000516	10:28	182.3	4.8	0.38

### 3.4 Selection of SAR scenes to compare with models

In order to compare the SAR derived wind speed maps with the mesoscale model results, it is also necessary to select a subset of the SAR scenes for which the wind speed measured at the mast is constant for at least a few hours and compares well with the surface wind speed at 10m height from the reanalysis data. This is because the mesoscale model cannot be expected to perform very well if the applied large scale forcing is not realistic. We exclude SAR scenes for which the wind speed difference exceeds  $3 \text{ m/s}$ . A typical example illustrating the selection procedure is depicted in Figure 3. It seen in the figure that the wind speed and direction measured at the mast is relatively close to the surface wind at 10m height from the reanalysis data. Also, temperature data from the mast is utilized to select scenes with reasonably constant Monin-Obukhov length to ensure constant atmospheric stability. Furthermore, as we do not want to simulate fronts in the mesoscale model, we have analyzed

weather charts from DWD [12] to exclude SAR scenes containing abrupt spatial changes in wind speed caused by fronts. It is important that the quality of the SAR data is independent of the above restrictions which have only been introduced to allow comparison with wind speed maps computed by the mesoscale model. The resulting selection consists of the scenes 4,7,8,9, and 13 (see Table I) which have been analyzed in the present work.

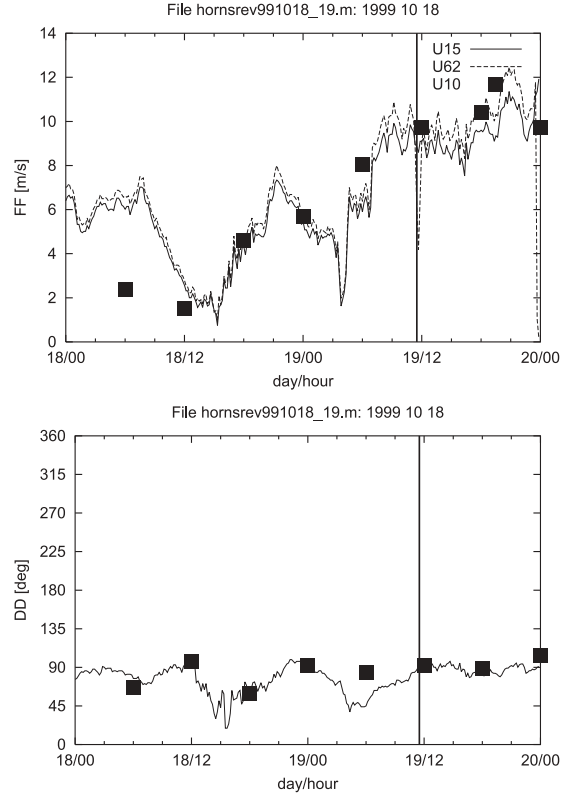


**Figure 3.** Wind speed (above) and wind direction (below) measured at the mast at Horns Rev compared to the surface wind at 10m height from the reanalysis data (filled boxes). The satellite overpassing corresponding to case 9 is indicated with a vertical line.

## 4 RESULTS AND DISCUSSION

The satellite SAR derived wind speeds and the mesoscale model results have been plotted together with the LINCOM results along a number of differently oriented transects. An example for case number 9, which has offshore wind and unstable atmospheric conditions, is shown in Figure 4 for the transect depicted in Figure 1. In the bottom of Figure 4 the corresponding sea depth is shown (zero depth corresponding to the coast). The transect position is shown at the x-axis. For this particular transect, we consider the SAR data unreliable for positions greater than 80 km (i.e. near the shore located at 92 km) because of tidal flats and surges. The first part of the SAR data show increasing wind speeds, as the distance to the coast decreases, which is not as significant in the mesoscale results and not produced by LINCOM. Near the 67 km position a sudden drop in the SAR derived wind speed is manifest. This sudden drop cannot be explained by the present mesoscale or LINCOM calculations, although the general trend and wind speed

level further out at sea has a good correspondence within the expected margins of error.

In some other investigated cases, similar increasing or decreasing trends and in addition oscillating behavior of the SAR derived wind speeds with transect position is observed. We believe these features may be caused by mechanisms similar to land-sea breezes driven by horizontal temperature gradients in the sea temperature or errors in the SAR derived wind speeds due to physical phenomena related to the fetch limitations.

The mesoscale model results are very similar for the two different horizontal resolutions of 1 km and 500 m, proving that grid independence is achieved for a resolution of 1 km. We find in general that a resolution of 1 km is sufficient for mesoscale calculations at Horns Rev.

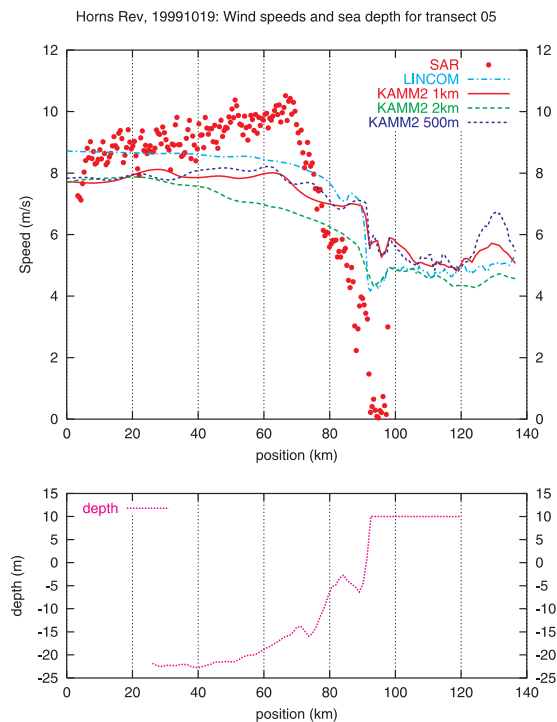


**Figure 4.** Wind speeds (above) derived from SAR compared to the corresponding mesoscale model results for three different horizontal resolutions and compared to the LINCOM results along the transect shown in Figure 1. Depths (below) extracted from a bathymetry from the Danish Hydraulic Institute.

## 5 CONCLUSION

A spatial comparison of satellite SAR derived wind maps to results from the mesoscale model KAMM2 and the linear spectral model LINCOM has been performed. The mesoscale model largely follow general trends in the SAR based wind maps. However SAR based wind maps capture features not present in the models.

Further analysis on wind streaks in the SAR scenes is under way. This will test against the wind directions measured at the mast. A number of scenes from other sites in Norway and Italy is being analyzed. This is to ensure the applicability of ERS SAR wind speed maps for offshore wind resource assessment under different atmospheric and climatic conditions.

## 6 ACKNOWLEDGEMENTS

The present work was funded by the EU project WEMSAR (Wind Energy Mapping using Synthetic Aperture Radar) ERK6-CT-1999-00017. Satellite data are from ESA AO3-153. Meteorological and marine data from Horns Rev are from ELSAM/ELTRA and tidal data in Esbjerg Harbour is from DMI/Farvandsvaesenet. Bathymetry from DHI/50395/2.ed.Nov-2001/PH/KAE.

## 7 REFERENCES

- [1] S. Neckelmann, J. Petersen, Evaluation of the stand-alone wind and wave measurement systems for the Horns Rev 150 MW offshore wind farm in Denmark. Proceedings to OWEMES 2000, Offshore wind energy in Mediterranean and other European Seas, (2000) 17-27.
- [2] G. Adrian, "Das Karlsruher Atmosphärische Mesoskalige Modell KAMM," Prof. Dr. Franz Fiedler zum 60. Geburtstag, VBIMK, **21**, editor K. D. Beheng, IMK, 1998, Karlsruhe, Germany.
- [3] G. Adrian and F. Fiedler, "Simulation of unstationary wind and temperature fields over complex terrain and comparison with observations," Beitr. Phys. Atmos., **64**, (1991) 27-48.
- [4] G. Adrian, "Zur Dynamik des Windfeldes über orographisch gegliedertem Gelände," Ber. Deutscher Wetterdienst, **188**, (1994) 1-142.
- [5] H. P. Frank, S. Larsen, and J. Højstrup, "Simulated Wind Power Off-shore Using Different Parametrizations for the Sea Surface Roughness," Wind Energ., **3**, 67-79 (2000).
- [6] NCEP Reanalysis data provided by the NOAA-CIRES Climate Diagnostics Center, Boulder, Colorado, USA, from their Web site at <http://www.cdc.noaa.gov/>
- [7] P. Astrup, N.O. Jensen, T. Mikkelsen, Surface Roughness Model for LINCOM. Risø National Laboratory, Denmark, Risø-R-900(EN) (1996)
- [8] P. Astrup, S.E. Larsen, WAsP Engineering Flow Model for Wind over land and Sea. Risø National Laboratory, Denmark, Risø-R-1107(EN), (1999)
- [9] Hasager, C.B., Furevik, B., Dellwik, E., Sandven, S. Frank, H.P., Jensen, N.O., Astrup, P., Joergensen, B.H., Rathmann, O., Barthelmie, R.; Johannessen, O., Gaudiosi, G.; Christensen, L.C., 2001 Satellite images used in offshore wind resource assessment. 2001 *Proceedings of the European Wind Energy Conference and exhibition (EWEC)*, Copenhagen (DK), 2-6 July 2001, 5 pages (in press).
- [10] Y. Quilfen, B. Chapron, T. Elfouhaily, K. Katsaros, & J. Tournadre, Observation of tropical cyclones by high-resolution scatterometry. J. Geophys. Research, **103**, **C4**, (1998) 7767-7786
- [11] A. Stoffelen, D.L.T. Anderson, Wind retrieval and ERS-1 scatterometer radar backscatter measurements. Advance Space Research, **13**, (1993) 53-60
- [12] DWD (1999-2000) European Meteorological Bulletin surface charts from DWD in resolutions 1:30.000.000 and 1:60.000.000. Deutscher Wetterdienst, Offenbach, Germany.